1989

Analysis of EPDM Terpolymers by Near-Infrared Spectroscopy and Multivariate Calibration Methods

Charles E. Miller
Haverford College

60° KRS-5 prism, the absorbance ratio was between 3 and 4, indicating that the 1730-cm^{-1} absorbance for the 150-mm^2 sample was only about half of what should have been measured. This low absorbance was probably due to the 60° KRS-5 prisms not optimally sampling the smaller sample size because of the lower number of internal reflections (5 vs. 12 reflections for the 45° prisms, see Table I).

Figure 4 shows the effect of pressure on absorbance with the use of the modified clamp. With a 45° KRS-5 prism, the 1730-cm^{-1} absorbance for the clearcoat surface rapidly increased with pressure to saturation for both the painted SMC and steel samples (Fig. 4A, curves 1 and 2). On the other hand, the 60° KRS-5 and 45° Ge prisms gave good results because both the 1730-cm^{-1} absorbances (Fig. 4A) and the 1730/815-cm^{-1} absorbance ratios (Fig. 4B) became relatively constant at pressures greater than 4 MPa for both the painted SMC and peeled paint samples. Even though sample CC/BC/CRS with a steel substrate required a higher pressure (about 10 MPa) before the absorbances leveled off (Fig. 4A, curve 5), the modified clamp has enabled us for the first time to reproducibly analyze clearcoat surfaces with the paint still on the steel substrate.

The efficacy of the clamp modifications can be seen by comparing the data in Figs. 3 and 4 for the peeled paint sample CC/BC with the 60° KRS-5 prism. The 1730-cm^{-1} absorbance obtained with the modified apparatus (Fig. 4A, curve 3) was twice that obtained with the clamp as received (Fig. 3A, bottom curve) and leveled off at 4 MPa rather than 12 MPa. The 1730/815-cm^{-1} absorbance ratio obtained with the modified clamp was much more constant over the entire measured pressure range than that obtained with the original clamp (Fig. 4B, curve 3, and Fig. 3B, top curve, respectively). The lower pressures to achieve maximum absorbance or constant absorbance ratio have extended crystal life by reducing KRS-5 distortion or Ge breakage.

Although a load cell was used in this study, its usage was not essential for reproducible sample-to-prism pressures with the modified clamp. Instead, a torque wrench may be used (we have used Utica Models TS-30 and TS-100), provided that the rotating contact points of the clamp screw are well lubricated and have low friction.

CONCLUSIONS

A modified clamp has improved the sample-to-prism contact for quantitative measurements of paint surfaces using internal reflection infrared spectroscopy. Maximum absorbances and constant absorbance ratios were obtained at reasonable sample-to-prism pressures with the use of the modified clamp and prism holder.

ACKNOWLEDGMENTS

The authors are grateful to W. R. Rodgers and R. E. Rudzinski for the paint samples, to G. L. Kilbertus for the load cell apparatus, and to members of the Processing Dept. for making the modified clamp.

1. D. J. McEwen, M. H. Verma, and R. O. Turner, J. Coatings Tech. **59 (755)**, 123 (Dec., 1987).
2. N. J. Harrick, *Internal Reflection Spectroscopy* (Harrick Scientific Corporation, New York, 1979), second printing.

Analysis of EPDM Terpolymers by Near-Infrared Spectroscopy and Multivariate Calibration Methods

CHARLES E. MILLER

Center for Process Analytical Chemistry, Department of Chemistry, BG-10, University of Washington, Seattle, Washington 98195

Near-infrared spectroscopy in the combination, first overtone, and second overtone regions is combined with the multivariate methods of Partial-Least-Squares (PLS) and Classical-Least-Squares (CLS) to provide calibrations for chemical components in ethylene-propylene-diene monomer (EPDM) terpolymers. EPDM samples with 1,4-hexadiene (HD) and ethylidene norbornene (ENB) diene monomers were used for this study. Because unknown interaction effects are present in the spectra of these materials, the PLS calibration method gives more accurate calibrations than the CLS method. PLS coefficient spectra and CLS reconstructed spectra obtained from the calibrations are used to determine the sources of the unknown spectral effects. Results indicate that the combination, first overtone, and second overtone regions of the spectrum can be used to determine ethylene and propylene concentrations in the terpolymers, and the combination region can be used to determine diene concentrations. The presence of intrachain and interchain interactions in the terpolymers is indicated by observation of CLS reconstructed spectra.

Index Headings: **Analysis for polymers; Near-infrared.**

INTRODUCTION

Ethylene-propylene-diene monomer rubbers (EPDMs) are used for many different applications, including automotive belts, hoses, and tires, nonautomotive hoses, and electrical insulation. These terpolymers are mostly composed of ethylene and propylene units, but also contain diene functionalities in the polymer backbone that are used to make crosslinks. Earlier studies have shown that important physical properties such as modulus, relaxation, and thermal transitions are greatly influenced by the composition of these polymers.[1,2]

Received 23 January 1989.

0003-7028/89/4308-1435$2.00/0

TABLE I. List of EPDM polymers.

Sample number	Concentrations (in mass %)			
	Ethylene	Propylene	ENB	HD
1	58	35	6.3	0
2	52	43	4.8	0
3	60	36	4.1	0
4	67	30	3.5	0
5	52	40	7.8	0
6	69	26	4.9	0
7	65	31	3.9	0
8	52	40	8.1	0
9	54	43	0	2.7
10	54	44	0	2.2
11	53	43	0	3.3
12	54	42	0	3.9
13	72	24	0	3.7
14	73.6	21.8	0	4.6

Because vibrational spectroscopy is very sensitive to the relative amounts of different functional groups in a sample, it is very useful for the determination of bulk composition of these polymers. Spectroscopy in the mid-infrared region (4000–600 cm^{-1}) is a valuable analytical method. However, it is rarely conducive to analysis of polymers without substantial sample preparation. In situations where a rapid quantitative analysis of raw polymer samples is desired, spectroscopy in the near-infrared (NIR) region[3,4] provides an alternative option.

Signals obtained from NIR spectroscopy are primarily vibrational combination and overtone bands. Because the absorptivities of these bands are orders of magnitude less than those of vibrational fundamental bands (observed in mid-IR spectra), thicker samples can be used in NIR analysis than in mid-IR analysis. As a result, rubber samples can be analyzed as films with thicknesses ranging from 0.1 mm to 10 cm.

Unfortunately, the spectral signals obtained from different C-H groups in EPDMs are highly overlapped in the NIR region. As a result, it is necessary to use as much spectral information as possible to separate the effects of different monomer units in the polymer. The multivariate methods of Classical-Least-Squares (CLS)[5,6] and Partial-Least-Squares (PLS)[5,7,8] can overcome the effects of overlapping analyte peaks, and thereby provide the means to determine composition using NIR spectra.

Earlier NIR analyses of ethylene-propylene co-polymer films[9–11] demonstrated the ability of NIR spectroscopy to determine chemical composition. However, these calibrations used only one or two absorbance bands at user-chosen wavelengths. Furthermore, only the combination region was used for these analyses. Improvements in NIR instrumentation and multivariate data analysis made after the earlier analyses have provided abilities both to improve calibrations and to use spectral regions other than the combination region for quantitative analysis. In this work, the multivariate methods of PLS and CLS will be used with NIR spectra in the combination, first overtone, and second overtone regions to predict chemical composition in EPDM polymers.

EXPERIMENTAL

Commercially available EPDMs were used in this analysis (labeled samples 1 to 14): samples 1–5 are Nitriflex EPDMs, samples 6–8 are Royalene EPDMs, and samples 9–14 are Nordel EPDMs. The diene unit used in the Nitriflex amd Royalene samples is 5-ethylidene bicyclo[2.2.1] hept-2-ene (or ethylidene norbornene, ENB), and the diene unit used in the Nordel samples was 1,4-hexadiene (HD). All samples were obtained as uncrosslinked polymers. Reference chemical composition values of the EPDM polymers were obtained by FT-NMR spectroscopy of the samples dissolved in $CDCl_3$. Estimated errors in the NMR composition values are 2% (mass) for ethylene and propylene, and 0.5% (mass) for ENB and HD. A complete list of the samples, with their NMR-determined compositions, is shown in Table I. All concentrations are expressed in mass percentages.

NIR spectra of the polymers were obtained with a Pacific Scientific 6250 near-infrared grating spectrophotometer with a lead-sulfide detector. The spectral range was 1100–2500 nm, the nominal resolution was 10 nm, and the wavelength reproducibility was ±1 nm. Each scan lasted about 30 s. Spectral data were saved on an IBM-AT microcomputer for later data processing.

The polymers were sampled by NIR in CCl_4 and as bulk samples. For the bulk sampling, a thin piece of material (approximately 1 mm thick) was cut and placed in a reflectance sample cup with a ceramic background and a quartz window. Reflectance spectra were obtained by illuminating the sample with NIR light and collecting back-scattered light. Each sample was analyzed in duplicate, with the use of two different pieces of the bulk sample.

EPDM solutions of approximately 5% (w/v) were prepared by placing approximately 0.2 g of polymer and 40 mL of CCl_4 (Aldrich) in an 80-mL vial. After 24 h, several samples had significant gel fractions. As a result, each solution was homogenized (Helvitica homogenizer) for approximately 30 s to disperse the nonsoluble portion of the polymer. The concentration of polymer in each solution was determined by pipetting 10 mL of the homogenized solution into a pre-weighed aluminum pan and weighing the pan again after solvent evaporation. The samples were then placed in a 4-mm-thick quartz cuvette and analyzed by NIR transmission spectroscopy. Spectra of pure CCl_4 solvent were then subtracted from the solution spectra.

NIR reflectance spectra of high-density polyethylene (HD-PE) (Aldrich) and isotactic polypropylene (*ISO*-PP) (Aldrich) were obtained by placing the samples in a standard reflectance cup with a quartz window. The HD-PE sample was obtained in pellet form, and had to be ground before NIR reflectance analysis.

Spectral data pretreatment consisted of one or two data corrections. The bulk sample spectra were corrected with Multiplicative Scatter Correction (MSC).[12] Each solution spectrum was corrected by subtracting the absorbance value at 1100 nm from all other absorbance values, and dividing the resulting absorbance values by the concentration of polymer in the sample (in g/10 mL). For both rubber and solution spectra, second-derivative correction (Pacific Scientific Co.) was sometimes used prior to subsequent correction methods.

The NIR spectra were split into three spectral regions: region 1 (1100–1350 nm), region 2 (1570–1850 nm), and region 3 (1950–2500 nm). Each region was used sepa-

rately for multivariate analysis. A PLS multivariate analysis program developed by the Center for Process Analytical Chemistry[7] was used. Mean-centered spectral data were used for all PLS analyses. CLS analyses were performed with a LOTUS-123 data spreadsheet.

THEORY

All multivariate analysis methods can utilize all available wavelengths in a spectrum to correlate to important properties of a system. However, PLS and CLS methods differ greatly in their approaches and, therefore, differ in the amount and type of information obtained. Previous work by Beebe and Kowalski[5] described the differences between these methods in detail.

CLS. In CLS calibration, spectra that are baseline-corrected and normalized to the product of the sample concentration and the spectroscopic pathlength are required. In addition, the number of different chemical components in the samples must be known, and concentration values for all chemical components for all samples must be known. In the CLS model, the chemical concentrations and spectral absorbance values are related by the Beer-Lambert equation

$$\mathbf{A} = \mathbf{KC} + \mathbf{E} \tag{1}$$

where $\mathbf{A}$ is an $n \times m$ matrix containing the spectral absorbances at n wavelengths for the m calibration samples, $\mathbf{C}$ is a $p \times m$ matrix containing concentrations of p chemical components for the m calibration samples, $\mathbf{K}$ is an $n \times p$ matrix containing the spectra of the p different pure components in the samples, and $\mathbf{E}$ is an $n \times m$ matrix of random spectral errors. Given $\mathbf{A}$ and $\mathbf{C}$, $\mathbf{K}$ can be estimated by the least-squares solution

$$\hat{\mathbf{K}} = \mathbf{AC}^t(\mathbf{CC}^t)^{-1}. \tag{2}$$

The columns in $\hat{\mathbf{K}}$ are the reconstructed analyte spectra or basis spectra, which are very useful for qualitative analysis. Estimated concentrations for all of the analytes in the calibration samples are determined by fitting the basis spectra ($\hat{\mathbf{K}}$) to each of the calibration spectra. The estimated concentrations are then plotted against the known concentrations to obtain calibration curves for the different analytes. Spectral residuals ($\mathbf{E}$) are useful for outlier sample detection and for determination of unknown spectral effects.

PLS. In PLS calibration, the calibration spectra are modeled according to Eq. 3:

$$\mathbf{A} = \mathbf{TP}^t + \mathbf{E} \tag{3}$$

where $\mathbf{P}$ is an $m \times f$ matrix containing f orthogonal spectral factors, or loadings, and $\mathbf{T}$ is an $n \times f$ matrix containing the scores of each factor for each calibration sample.[5] The $\mathbf{A}$ matrix contains the calibration spectra, and the $\mathbf{E}$ matrix contains spectral residuals. The calibration spectra in $\mathbf{A}$ must be normalized with respect to the product of the sample concentration and spectroscopic pathlength before PLS calibration. In this work, only one analyte is calibrated for each PLS calibration.

The spectral factors in $\mathbf{P}$ describe relevant spectral variations and are useful for qualitative analysis. The scores ($\mathbf{T}$) are used to determine estimated concentrations of the analyte in the calibration samples, which can be used to construct a calibration curve. In addition, a PLS coefficient spectrum can be constructed from the $\mathbf{T}$ and $\mathbf{P}$ matrices. Because the coefficient spectrum indicates wavelengths that are important for quantitation of the analyte, it is also very useful for qualitative analysis.

The appropriate number of factors (f) in a PLS calibration can be determined by the method of cross-validation.[7,13] In cross-validation, the calibration samples are split into a calibration set and prediction set. PLS calibrations using different numbers of factors are constructed from the calibration samples and used to predict concentrations of an analyte in the prediction samples. The optimal number of factors can then be determined from observation of the prediction errors as a function of the number of factors in the PLS calibration.

CLS vs. PLS. The review article by Beebe and Kowalski[5] discusses the differences between PLS and CLS calibration methods (in Ref. 5, CLS is referred to as MLR). In CLS calibration, the presence of irrelevant spectral variations (from chemical interactions or unknown chemical components in the calibration samples) worsens the calibration performance. In PLS calibration, only spectral variations that are relevant to the quantitation of the analyte are used. As a result, PLS outperforms CLS when unknown spectral variations are present. However, one must avoid overfitting of PLS calibrations by the use of too many spectral factors.

If unknown spectral effects are not too large, the CLS method is expected to yield better qualitative information. The CLS basis spectra are the closest possible approximation to the spectra of the pure chemical components in the samples.

Prediction Ability of Calibrations. The prediction ability of CLS and PLS calibrations is estimated by a "leave-one-out" cross-validation procedure. For each calibration, a prediction error for each calibration sample is determined by constructing a calibration with all other samples and using it to predict the concentration of analyte in the "left-out" sample. After all of the samples have been "left-out" and predicted, the standard error of prediction (SEP) is calculated:

$$\mathrm{SEP} = \left[\frac{\sum_{i=1}^{N}(c_i - \hat{c}_i)^2}{N-1}\right]^{1/2} \tag{4}$$

where $\hat{c}_i$ is the predicted concentration of analyte in sample i, c_i is the known concentration, and N is the number of calibration samples.

Chemical Interaction in EPDMs. Although the monomer units in EPDM polymers (ethylene, propylene, ENB, and HD) were covalently bonded in the polymer chains, they were considered as separate chemical components in the polymers. Interactions between these components can be of two types: intrachain and interchain.

Intrachain interactions involve adjacent monomer units in a polymer chain. For example, differences in the infrared spectra of block and random ethylene-propylene co-polymers were observed[11] because the vibrational spectroscopy of the ethylene and propylene groups is sensitive to the identities of adjacent groups in the poly-

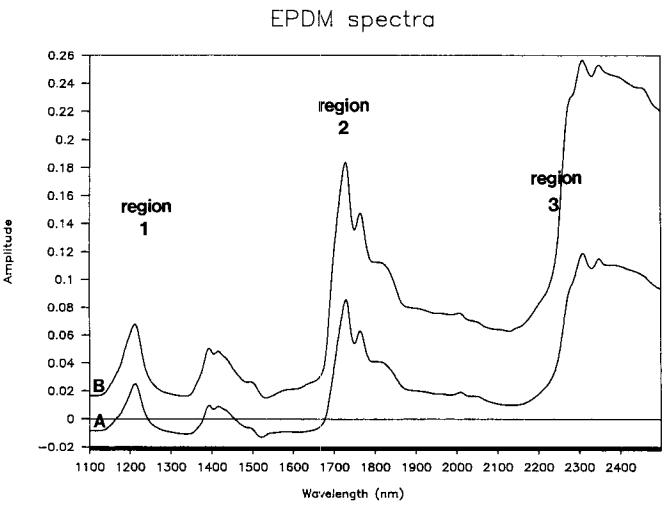

FIG. 1. Near-infrared reflectance spectra of bulk EPDM sample 14 (A) and sample 2 (B). Region 1 is 1100–1350 nm, region 2 is 1570–1850 nm, and region 3 is 1950–2500 nm.

mer chain. Interchain interactions occur between monomer units that are not adjacent in the same polymer chain. Polymer crystallinity and morphology are a result of interchain interactions.

Because both intrachain and interchain interactions have been found to affect infrared spectra of polymers,[9,11] they are also expected to affect the near-IR spectra of polymers. The nature and extent of these interactions for the EPDM samples used in this work were not known before multivariate analysis.

RESULTS

NIR reflectance spectra of a high-ethylene and low-ethylene EPDM elastomer are shown in Fig. 1. Regions of significant absorption are designated as region 1 (1100–1350 nm), region 2 (1570–1850 nm), and region 3 (1950–2500 nm). Although significant absorptions are found in the region 1350–1570 nm, instrumental anomalies in this region prevent its use for quantitative analysis. Regions 1, 2, and 3 are used separately for multivariate analysis because they have different NIR sampling characteristics. Region 1 is dominated by second overtone C-H stretching bands. The low absorptivities of these bands permit the use of this region for the sampling of thick films (up to several cm thick) and large pellets. Region 2 is dominated by first-overtone C-H stretching bands, which have about an order-of-magnitude higher absorptivity than the bands in region 1. As a result, region 2 can be used for thinner films (about 0.5–2 mm thick) and dilute solutions. Region 3 contains C-H combination bands with much higher absorptivities than those of the bands in regions 1 and 2. This region is appropriate for very thin films (less than 0.1 mm thick) and dilute solutions. Because the bulk samples were approximately 1 mm thick, region 3 was not useful for bulk EPDM analysis. However, this region was useful for dilute EPDM solutions.

Although sampling difficulty increases as one goes from region 1 to region 3, spectral information and spectral resolution increase also. Unlike the overtone bands in regions 1 and 2, the combination bands in region 3 are affected by fundamental vibrations in the low-energy (approximately 600–2000 cm^{-1}) IR spectrum, and therefore contain much more information than do the former regions.

A consequence of rapid sampling of EPDM elastomers with NIR spectroscopy is the presence of baseline shifts and differences in absolute peak amplitudes in the spectra (see Fig. 1), which are results of nonreproducible NIR sampling. The baseline offset effect is a function of sample placement in the spectrometer, and the peak amplitude effect is a function of the product of sample concentration and spectral pathlength (or sample thickness). Because the CLS and PLS methods perform better with spectra that are baseline-corrected and normalized to the product of sample concentration and spectral pathlength, MSC spectral correction was applied to the bulk spectra.

TABLE II. CLS prediction errors.

Spectral region	Data correction[a]	Analyte SEP (in mass %) Ethylene	Propylene	ENB	HD
EPDM solutions:					
1	Normal	3.6	5.3	9.1	5.2
1	2nd deriv.	3.9	4.0	6.1	5.2
2	Normal	2.9	3.2	4.0	4.1
2	2nd deriv.	2.3	2.1	4.2	2.4
3	Normal	2.5	3.8	5.0	2.0
3	2nd deriv.	2.2	4.5	2.8	2.2
Bulk EPDM:					
1	MSC	5.9	11	8.9	5.6
1	MSC-2D	6.5	5.9	12	2.3
2	MSC	2.9	4.5	5.1	2.3
2	MSC-2D	3.4	2.9	5.6	3.8

[a] Normal: subtraction of baseline at 1100 nm and normalization to solution concentrations only; 2nd deriv.: second-derivative correction, then normalization to solution concentration; MSC: Multiplicative Scatter Correction (see Ref. 12); MSC-2D: second-derivative correction, then Multiplicative Scatter Correction.

TABLE III. Cross-validation results.

Prediction set 1: Samples: 4, 5, 7, 11, 13
Prediction set 2: Samples: 3, 6, 8, 9, 12

Number of times a given optimal number of factors was determined by cross-validation

Spectral region	Data correction[a]	Number of factors 1	2	3	4	5
EPDM solutions:						
1	Normal	1	3	2	2	0
2	Normal	0	1	5	2	0
3	Normal	0	5	2	1	0
1	2nd deriv.	4	2	1	1	0
2	2nd deriv.	0	4	4	0	0
3	2nd deriv.	2	2	3	1	0
Bulk EPDM samples:						
1	MSC	0	1	2	2	3
2	MSC	0	1	3	3	1
1	MSC-2D	0	1	0	5	2
2	MSC-2D	0	1	3	4	0
All EPDM solution calibrations:		7	17	17	7	0
All bulk EPDM calibrations:		0	4	8	14	6

[a] Same abbreviations as in Table II.

Second-derivative correction was also applied to both the bulk elastomer and solution spectra. Second-derivative correction eliminates baseline offset and improves spectral resolution. However, it also increases spectral noise and produces spectra that are difficult to interpret qualitatively.

CLS Results. Table II lists the leave-one-out SEP values of CLS calibrations for EPDM rubber and solution samples. Second-derivative spectral correction improved the results of many calibrations, but worsened the results for some calibrations. In most cases, the SEP values were noticeably reduced as the spectral region changed from region 1 to region 2 (to region 3, for the solution samples). The spectral information content and spectral resolution increase as one moves from region 1 to region 3; this trend is reflected in the prediction results.

The SEP values for ethylene and propylene were, for the most part, slightly greater than the estimated error of the reference NMR method for ethylene and propylene concentration (2%). SEP values for ethylene were generally below 4% (mass) and SEP values for propylene were below 6%.

The prediction errors for ethylene and propylene in bulk EPDM elastomers were much higher than the prediction errors for these analytes in their solutions. This difference could have been caused by inadequate removal of sampling effects from the bulk polymer spectra, or by the presence of unknown spectral effects for the bulk samples that were not present in the solution spectra.

Predictions of ENB and HD in EPDM are expected to be more difficult than those for ethylene and propylene, because the concentrations of these monomer units are much lower than the concentrations of ethylene and propylene units (see Table I). In addition, there are few functional groups in these monomer units that can give unique spectral signals, especially at low spectral resolution. Region 3, which has the best spectral resolution and most information of all three regions, provides the best possibility for quantitative analysis of ENB and HD. The errors for ENB and HD calibrations in region 3 were within 35–65% of the range of concentration values of these analytes in the samples.

PLS Results. The first step in all PLS calibrations was the determination of the optimal number of spectral factors. If all chemical components are known, and there are no interactions between them, the optimal number of factors for PLS calibrations using mean-centered EPDM spectra is three, because there are four different chemical components in the polymers (ethylene, propylene, ENB, and HD units). However, additional factors might be necessary in order to explain unknown spectral components. In an attempt to determine a more reliable number of factors for PLS calibrations, cross-validations were performed with each PLS calibration with the use of two user-selected prediction sets (see Table III). The most frequently chosen optimal numbers of factors are two and three for the solution calibrations and four for the bulk elastomer calibrations. The lack of conclusive results could have been caused by the small number of samples (fourteen) or by the experimental design.

The cross-validation results suggest that at least three factors should be used in all PLS calibrations, and perhaps four factors should be used in the bulk elastomer calibrations. Because there are four known chemical components in the samples that are spectroscopically active, the use of three factors in PLS calibrations should not result in overfitting. With these considerations in mind, three factors were used in all PLS calibrations with the solution spectra, and four factors were used in all calibrations with the bulk spectra.

TABLE IV. PLS prediction errors.

Spectral region	Data correction[a]	Analyte SEP (in mass %)			
		Ethylene	Propylene	ENB	HD
EPDM solutions:					
1	Normal	3.7	5.0	3.7	2.4
1	2nd deriv.	2.7	3.8	2.7	2.0
2	Normal	1.9	1.6	3.0	2.2
2	2nd deriv.	1.7	1.7	3.0	2.0
3	Normal	1.4	2.4	2.4	1.6
3	2nd deriv.	1.6	2.5	1.4	1.3
Bulk EPDM:					
1	MSC	1.9	1.9	2.6	1.7
1	MSC-2D	1.8	1.7	1.8	1.4
2	MSC	1.6	1.7	1.8	1.3
2	MSC-2D	1.7	1.7	1.0	1.0

[a] Same abbreviations as in Table II.

The SEP results of the PLS calibrations are shown in Table IV. For the most part, SEP values for PLS calibrations were significantly lower than the SEP values for CLS calibrations (Table II). The use of second-derivative-corrected spectra improved calibrations in most cases.

The large difference between calibration results from CLS and PLS suggested that there were unknown spectral variations in the EPDM solution and bulk spectra. These unknown spectral effects could have resulted from interchain or intrachain interactions in the polymers. It is possible that the NIR spectra of EPDMs are affected by varying amounts of block and random segments (or intrachain interactions) in the different polymers. Another possible effect, present only for the elastomer samples, is the effect of morphology, or interchain interactions. EPDM terpolymers with high ethylene contents can have significant crystallinity.[14,15] It is probable that crystallinity also affects the NIR spectra of these substances.

For the EPDM solution calibrations, many ethylene and propylene prediction errors were below the estimated error of the NMR reference method. Because the SEP values cannot be less than the actual error in the reference method, it is suspected that the estimated error in the NMR reference method is too high. The PLS calibrations for ENB and HD in region 3 were greatly improved relative to the CLS calibrations. The results for the PLS calibrations with the bulk samples are also very encouraging. The relatively low SEP values for the calibrations in region 1 are particularly noteworthy, because this region is tolerant of wide sample variations.

DISCUSSION

Multivariate calibration methods like PLS and CLS not only provide better calibration results than univariate methods but also provide qualitative information about the chemical system analyzed. In many cases, this

TABLE V. Sum of squares of spectral residuals—times 1000 (percent sum of squares of spectral residuals).

Spectral region	Data correction[a]	PLS calibrations				CLS calibration
		Ethylene	Propylene	ENB	HD	
EPDM solutions:						
1	Normal	0.22 (1.9)	0.23 (1.9)	0.36 (3.0)	0.46 (3.8)	0.44
1	2nd deriv.	0.18 (5.0)	0.19 (5.4)	0.18 (4.9)	0.17 (4.8)	0.20
2	Normal	1.8 (4.8)	1.9 (4.8)	2.0 (5.1)	2.0 (5.2)	2.3
2	2nd deriv.	1.5 (2.9)	2.1 (4.1)	2.3 (4.4)	1.8 (3.6)	1.7
3	Normal	18 (1.7)	21 (2.0)	22 (2.1)	26 (2.5)	28
3	2nd deriv.	8.2 (0.90)	7.7 (0.84)	7.8 (0.85)	7.8 (0.85)	14.7
Bulk EPDM:						
1	MSC	0.0090 (0.25)	0.010 (0.30)	0.012 (0.32)	0.039 (1.1)	0.34
1	MSC-2D	0.014 (2.7)	0.0084 (1.6)	0.014 (2.7)	0.014 (2.7)	0.93
2	MSC	0.32 (0.89)	0.24 (0.67)	0.35 (0.97)	0.34 (0.93)	0.75
2	MSC-2D	0.095 (1.9)	0.096 (1.9)	0.091 (1.8)	0.09 (1.8)	0.35

[a] Same abbreviations as in Table II.

qualitative information can be used to explain trends or inconsistencies in the quantitative analyses.

Spectral Residuals. In CLS and PLS calibrations, all variations in the calibration spectra must be explained in order to obtain an optimal calibration. The variations in the calibration spectra that are not explained by the multivariate model are called the spectral residuals. The specific quantity commonly used to refer to spectral residuals is the residual sum of squares (abbreviated "residual SS"), defined by the equation

$$\text{residual SS} = \sum_{i=1}^{N}\sum_{j=1}^{m}(a_{ij} - \hat{a}_{ij})^2 \qquad (5)$$

where a_{ij} and $\hat{a}_{ij}$ are the spectral absorbance values of sample i at wavelength j for the real calibration spectrum and the calibration spectrum modeled by the multivariate method, respectively. A zero residual indicates that all spectral variations (including noise) are modeled by the multivariate calibration. A large spectral residual can be caused by low signal-to-noise ratio in the spectral region used for the calibration, or by the presence of spectral effects not modeled by the calibration method.

Table V lists the residual SS for all of the PLS and CLS calibrations and the percent residual SS for the PLS calibrations. The percent residual SS is the residual SS divided by the sum-of-squares of the mean-centered calibration spectra. Note that only one residual value is reported for each CLS calibration, because all four analytes are calibrated in the same procedure. For the PLS calibrations in this work, one calibration model was constructed for each analyte.

The residuals for CLS calibrations are consistently higher than the residuals for corresponding PLS calibrations. This result is a further indication that significant spectral effects explained by the PLS calibration are not explained in the CLS calibrations. Of particular note is the large difference in spectral residuals for PLS and CLS calibrations with bulk samples. This difference corresponds to a large difference in prediction errors (see Tables II and IV). Earlier, it was mentioned that crystallinity could have affected the spectra of the bulk samples. It is probable that this effect, if it exists, is not accounted for by the CLS calibrations.

Comparison of PLS calibrations with different spectral data corrections and different spectral regions requires the use of percent residual SS values (the values in parentheses in Table V). For the PLS solution calibrations, second-derivative correction caused a decrease in percent residual SS values for regions 2 and 3, but caused an increase in percent residual SS values for region 1 calibrations. Despite this discrepancy, the prediction errors for all regions were slightly improved or unchanged by the use of second-derivative correction (Table IV). For regions 2 and 3, the deconvolution and baseline correction abilities of second-derivative correction dominated, and caused improved calibration fit and decreased spectral residuals. In region 1, where the signal-to-noise ratio was much less than in regions 2 and 3, the noise increasing effect of second-derivative correction became significant, which caused the spectral residuals to increase despite slight improvements in calibration results.

Qualitative Information. The CLS basis spectra (or reconstructed pure component spectra) and PLS coefficient spectra yield important qualitative information about the EPDM solutions and elastomers. For this discussion, spectra corrected with the second-derivative-

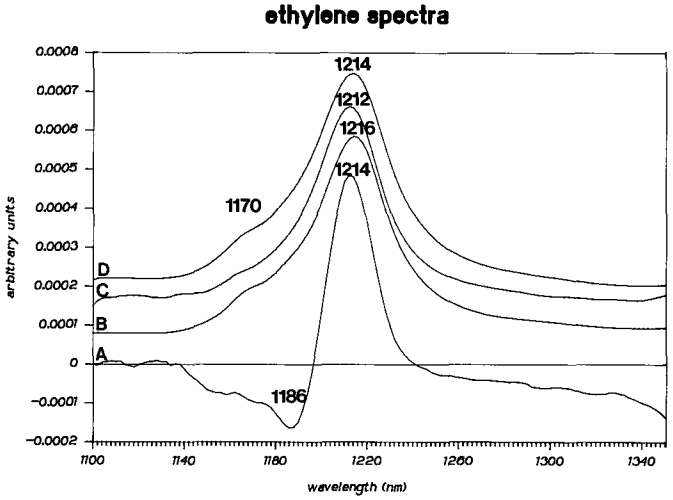

FIG. 2. (A) PLS coefficient spectrum of ethylene in EPDM solution; (B) NIR reflectance spectrum of high-density polyethylene; (C) CLS reconstructed spectra of ethylene in EPDM solution; (D) CLS reconstructed spectrum of ethylene in bulk EPDM in region 1. Spectra B, C, and D were vertically offset and scaled for clarity; spectrum A was only scaled for clarity.

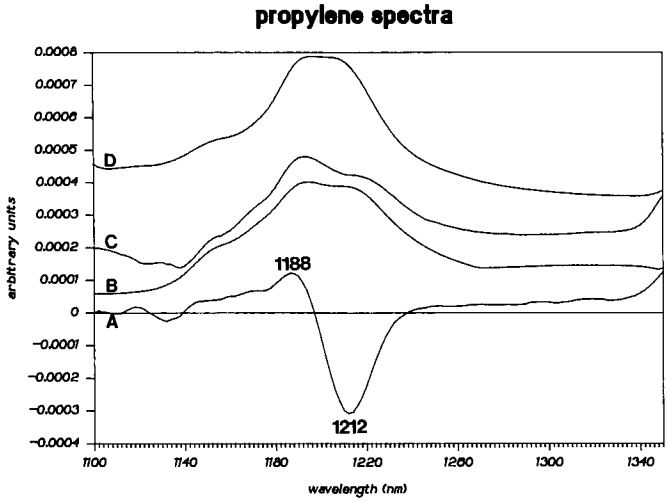

FIG. 3. (A) PLS coefficient spectrum of propylene in EPDM solution; (B) NIR reflectance spectrum of isotactic polypropylene; (C) CLS reconstructed spectra of propylene in EPDM solution; (D) CLS reconstructed spectrum of propylene in bulk EPDM in region 1. Offset and scaling were similar to that of Fig. 2.

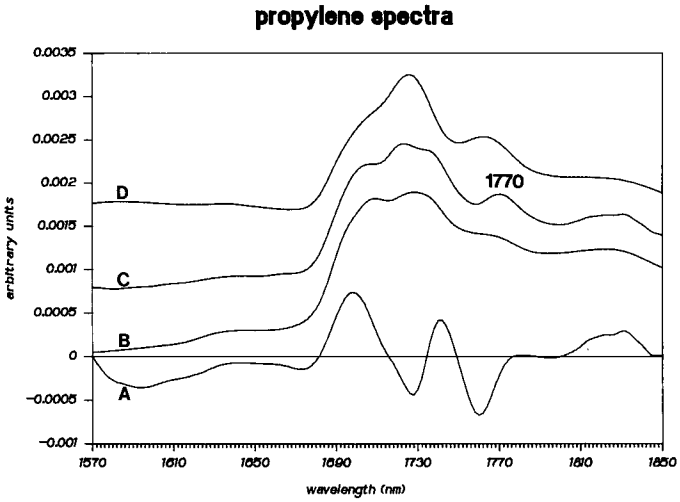

FIG. 5. (A) PLS coefficient spectrum of propylene in EPDM solution; (B) NIR reflectance spectrum of isotactic polypropylene; (C) CLS reconstructed spectra of propylene in EPDM solution; (D) CLS reconstructed spectrum of propylene in bulk EPDM in region 2. Offset and scaling were similar to that of Fig. 2.

corrected operation will not be used, because they are more difficult to interpret qualitatively.

Figure 2 shows the region 1 CLS reconstructed spectra of ethylene in EPDM solution (C) and in bulk (D), the PLS coefficient spectrum for ethylene in EPDM solution (A), and an NIR reflectance spectrum of high-density polyethylene (HD-PE) (B). Note that the CLS reconstructed spectra (C and D) closely resemble the spectrum of HD-PE (B). The difference between the CLS reconstructed spectra for ethylene in EPDM solution (C) and in bulk (D) is small, but significant. The reconstructed spectrum from the solutions had a peak maximum at 1212 nm, and the reconstructed spectrum from the bulk had a peak maximum at 1214 nm, which is closer to the peak maximum for HD-PE (1216 nm). Because the wavelength reproducibility of the NIR instrument is ±1 nm, these peak shifts are significant. In addition, a very small

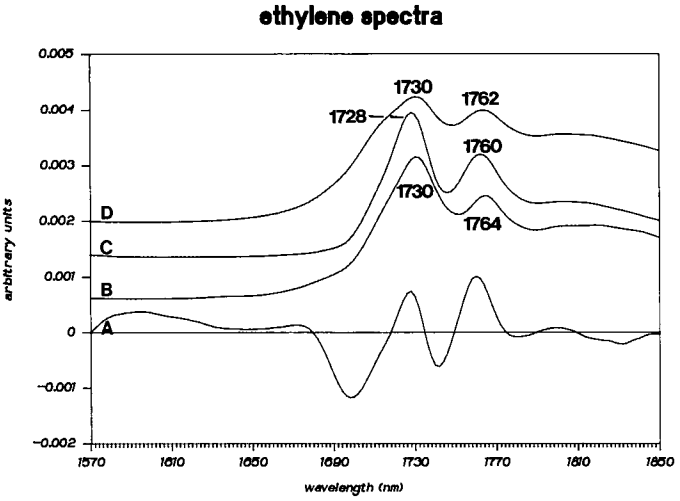

FIG. 4. (A) PLS coefficient spectrum of ethylene in EPDM solution; (B) NIR reflectance spectrum of high-density polyethylene; (C) CLS reconstructed spectra of ethylene in EPDM solution; (D) CLS reconstructed spectrum of ethylene in bulk EPDM in region 2. Offset and scaling were similar to that of Fig. 2.

shoulder at 1170 nm was observed only in the reconstructed spectrum from the elastomers (D) and in the HD-PE spectrum (B). These observations suggest that the ethylene units in EPDM elastomers were arranged more like the ethylene units in HD-PE than the ethylene units in EPDM solutions. If one assumes that HD-PE is highly crystalline, and the EPDM polymers do not exhibit crystallinity in solution, these results suggest that the ethylene units in the EPDM elastomers have significant crystallinity.

The PLS coefficient spectrum for ethylene in EPDM solution (Fig. 2, A) also resembles the spectrum of HD-PE (B), except for the negative peak at 1186 nm. This negative peak is most likely caused by the presence of propylene absorbance bands overlapping with the ethylene band. Its presence indicates that interfering propylene absorbances were accounted for in the ethylene calibration.

Figure 3 shows the CLS reconstructed spectra for propylene in EPDM solution (C) and in bulk (D), the PLS coefficient spectrum for propylene in EPDM solution (A), and the NIR reflectance spectrum of isotactic polypropylene (*ISO*-PP) (B). As is the case for ethylene, the two CLS reconstructed spectra closely resemble the spectrum of the homopolymer (*ISO*-PP). However, slight differences between the reconstructed spectra and the *ISO*-PP spectrum are observed. These differences might be caused by differences in intrachain interactions of the propylene units in the two polymer systems. In *ISO*-PP, the propylene units are connected in an ordered "head-to-tail" configuration. In EPDM polymers, the propylene units might be isolated between ethylene units in the chain, or arranged randomly in "head-to-head" and "head-to-tail" configurations in propylene blocks. This difference should cause a difference in the NIR spectrum of the propylene group in the two substances. The crystallinity effect, discussed earlier, might contribute to the observed deviations of the reconstructed spectrum in bulk EPDM (D) from the reconstructed spectrum of propylene in EPDM solution (C). Although the propylene

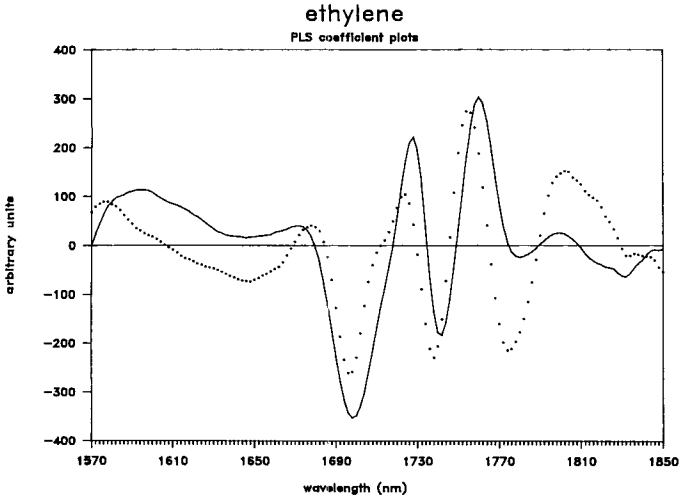

FIG. 6. PLS coeficient spectra for ethylene in EPDM solution (solid line) and in EPDM rubber (dotted line), in region 2.

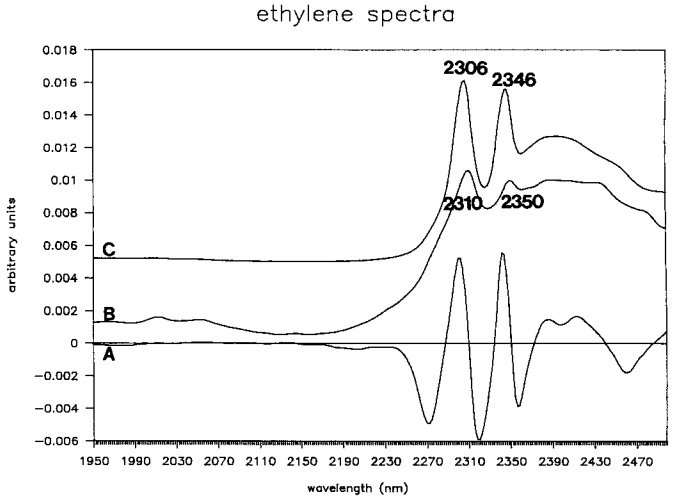

FIG. 7. (A) PLS coefficient spectrum of ethylene in EPDM solution; (B) NIR reflectance spectrum of high-density polyethylene; (C) CLS reconstructed spectra of ethylene in EPDM solution in region 3. Offset and scaling were similar to that of Fig. 2.

units in EPDM elastomers do not exhibit crystallinity themselves, they can be incorporated into crystalline domains of ethylene units,[14] thus causing their spectral properties to differ from those of propylene units in solution.

The PLS coefficient spectrum for propylene in EPDM solutions (Fig. 3, A) is almost exactly opposite to the PLS coefficient spectrum for ethylene (Fig. 2, A). A positive peak at 1188 nm indicates propylene absorption, and the negative peak at 1212 nm compensates for overlapping absorption from ethylene units.

Figures 4 and 5 are the region 2 analogs of Figs. 2 and 3. Note the shift in peak maxima between the CLS reconstructed spectrum for ethylene in EPDM solution (Fig. 4, C) and the spectrum of HD-PE (Fig. 4, B). The magnitude and direction of this shift are identical to those for region 1 mentioned earlier. This further indicates the large difference in morphology of ethylene units in EPDM solutions and in HD-PE. The reconstructed spectrum for ethylene in EPDM rubber (D) has peak maxima at approximately the same position as for HD-PE (1730 nm and 1762 nm). However, the peak at 1730 nm is much less intense than expected. This effect is probably caused by the nonlinear behavior of the strong ethylene band at 1730 nm, which resulted from the use of bulk samples that were too thick, or too absorbing.

The CLS reconstructed spectrum of propylene in EPDM solution (Fig. 5, C) and the *ISO*-PP spectrum (B) are very similar, but they do show small differences. For example, the peak at 1770 nm in the reconstructed spectrum in EPDM solution (C) is not present in the *ISO*-PP spectrum. As mentioned earlier, these differences could be caused by differences in intrachain and interchain interactions between propylene units in *ISO*-PP and in EPDM solution. The reconstructed spectrum of propylene in EPDM elastomer (D) differs greatly from the *ISO*-PP spectrum, much of which is likely caused by the nonlinear absorbance at 1730 nm.

The nonlinear absorbance at 1730 nm is considered to be caused by an unknown spectral effect, which should increase the number of independent spectral variations by one. PLS can explain the extra spectral effect more easily than CLS. This assertion is reflected in the CLS and PLS calibration results for EPDM elastomers, and in the spectral residuals of the CLS and PLS calibrations for the bulk elastomers in region 2 (Table V). In addition, the PLS coefficient spectra for ethylene in EPDM elastomers and solutions (Fig. 6) reflect the presence of nonlinearities. The PLS coefficient spectrum for ethylene in bulk EPDM shows much less intensity in the suspected nonlinear region (around 1730 nm) than the coefficient spectrum for ethylene in solution. Because the solution spectra are not expected to exhibit nonlinear behavior, this discrepancy is probably a result of nonlinear absorbances of the bulk samples in the region 1718 to 1730 nm. In effect, PLS corrected for the nonlinear spectral region by minimizing the effect of the region on the calibration. On the other hand, the CLS reconstructed spectrum (Fig. 4, D) gave a significant weight to the nonlinear region, which demonstrates the inability of CLS to correct for the nonlinear effects.

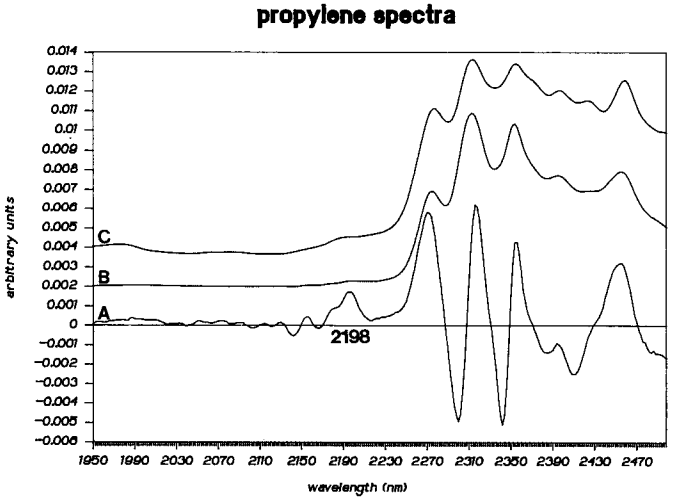

FIG. 8. (A) PLS coefficient spectrum of propylene in EPDM solution; (B) NIR reflectance spectrum of isotactic polypropylene; (C) CLS reconstructed spectra of propylene in EPDM solution in region 3. Offset and scaling were similar to that of Fig. 2.

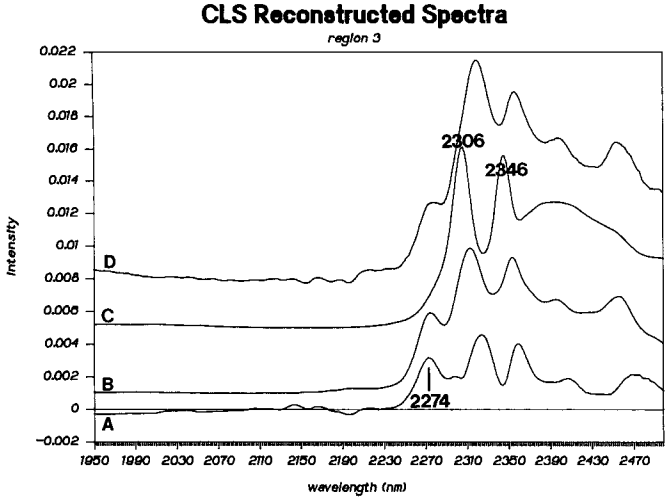

FIG. 9. CLS reconstructed spectra of ENB (A), propylene (B), ethylene (C), and HD (D). Spectra were offset for clarity.

Figures 7 and 8 are the region 3 analogs of Figs. 2 and 3. The CLS reconstructed spectrum for ethylene in EPDM solution (Fig. 7, C) is very similar to the HD-PE spectrum (B). As in regions 1 and 2, the major ethylene peaks (at 2310 and 2350 nm) are shifted to lower wavelength for the reconstructed spectrum of ethylene in EPDM solution. This result further indicates the large difference in morphology and intrachain interactions of ethylene units in EPDM solutions and in HD-PE. The PLS coefficients for ethylene in EPDM solution showed positive features where ethylene peaks exist and negative peaks where interfering absorptions exist. Small but significant differences between the CLS reconstructed spectrum of propylene in EPDM solution (Fig. 8, C) and the *ISO*-PP spectrum (B) are also observed. As mentioned earlier, this difference is the result of differences in interactions for propylene units in *ISO*-PP and in EPDM solution.

The PLS coeficient spectrum for propylene (Fig. 8, A) is almost an exact opposite of the PLS coefficient spectrum for ethylene, with the exception of a major positive feature at 2198 nm. This feature is slightly visible in the CLS reconstructed spectrum of propylene in EPDM solution (Fig. 8, C) and the *ISO*-PP spectrum (B). However, it is probably free of interferent peaks, and was therefore weighted highly in the PLS calibration. In this case, the PLS regression method demonstrates that the best absorbances used for calibration of an analyte are not necessarily the strongest analyte peaks, but the peaks with fewest interferences from other components.

In region 3, spectral resolution was much better than in regions 1 and 2. As a result, calibrations were greatly improved for all four analytes. The CLS reconstructed spectra for all four analytes in EPDM solution are shown in Fig. 9. A peak at 2274 nm, present in the reconstructed spectra of propylene, ENB, and HD, has been previously assigned as a methyl combination band.[11] The relative number of methyl groups per monomer unit in the three monomers decreases as one goes from propylene to HD to ENB; this trend is reflected in the intensity above baseline of the 2274-nm band in the three reconstructed spectra A, B, and D. Weak but significant bands are observed in the region 2130 to 2200 nm only for the ENB and HD reconstructed spectra. These bands are characteristic of unsaturation,[16] which is only present in the HD and ENB units. Absorptions from methylene and methyne groups in the polymer are observed in the region 2290 to 2450 nm. The most prominent of these are the 2306- and 2346-nm bands in the reconstructed spectrum of ethylene, which were previously assigned to ethylene group vibrations.[11]

CONCLUSIONS

NIR spectroscopy can be used to rapidly sample EPDM elastomers and solutions. This work has shown that the full potential of NIR for quantitative analysis cannot be realized unless multivariate calibration methods are used. Unlike univariate, or two-wavelength calibrations used earlier, PLS and CLS methods can account for overlap between analyte signals. Also, PLS can account for unknown interferents and spectral effects. Not only do PLS and CLS provide better quantitative results, but they also provide important qualitative information, which is observed in PLS coefficient spectra and CLS reconstructed analyte spectra. This additional information can be used to verify the presence of spectral interactions, interferents, and nonlinearities, and to improve the confidence of calibrations.

ACKNOWLEDGMENTS

I would like to thank the Goodyear Tire and Rubber Company for organizing a 1988 summer internship, during which the data were collected. Specific acknowledgments go to Jim Hermiller and Dr. Tom Gurley, for helpful guidance and suggestions. I also thank the NMR lab at Goodyear, specifically Lori Cianchetti, for essential lab analyses. Additional comments from Dr. Bruce E. Eichinger, Dr. Bruce R. Kowalski, and the Laboratory For Chemometrics at the University of Washington were greatly appreciated.

1. K. C. Baranwal and G. A. Lindsay, Rubber Chem. Tech. **45,** 1334 (1972).
2. M. C. Kirkham, J. Appl. Poly. Sci. **17,** 1101 (1973).
3. E. Stark, K. Luchter, and M. Margoshes, Appl. Spectrosc. Rev. **22,** 335 (1986).
4. L. G. Weyer, Appl. Spectrosc. Rev. **21,** 1 (1985).
5. K. Beebe and B. R. Kowalski, Anal. Chem. **59,** 1007A (1987).
6. D. M. Haaland, R. G. Easterling, and D. A. Vopicka, Appl. Spectrosc. **39,** 73 (1988).
7. D. Veltkamp and B. R. Kowalski, *PLS-2 Block Modeling, Version 1.9* (IBM) (Center for Process Analytical Chemistry, Seattle, Washington, 1986).
8. P. Geladi and B. R. Kowalski, Anal. Chim. Acta. **185,** 1 (1986).
9. R. M. Bly, P. E. Kiener, and B. A. Fries, Anal. Chem. **38,** 217 (1966).
10. T. Takeuchi, S. Tsuge, Y. Sugimura, Anal Chem. **41,** 184 (1969).
11. H. V. Drushel and F. A. Iddings, Anal. Chem. **35,** 28 (1963).
12. P. Geladi, D. MacDougall, and H. Martens, Appl. Spectrosc. **39,** 491 (1985).
13. D. M. Haaland and E. V. Thomas, Anal. Chem. **60,** 1193 (1988).
14. M. Gilbert, J. E. Briggs, and W. Omana, Br. Poly. J. **11,** 81 (1979).
15. C. K. Shih and E. F. Cluff, J. Appl. Poly. Sci. **21,** 2885 (1977).
16. R. F. Goddu, Anal. Chem. **29,** 1790 (1957).